Supporting Information

Improving the electrochemical performance of layered lithium-rich cathode material by fabricating a spinel outlayer with Ni^{3+}

Cheng Yang,Qian Zhang, Weixiang Ding, Jun Zang, Ming Lei, Mingsen Zheng* and Quanfeng Dong*

Department of Chemistry, College of Chemistry and Chemical Engineering,

Xiamen University,

State Key Laboratory of Physical Chemistry of Solid Surfaces,

Xiamen, Fujian, 361005, China.

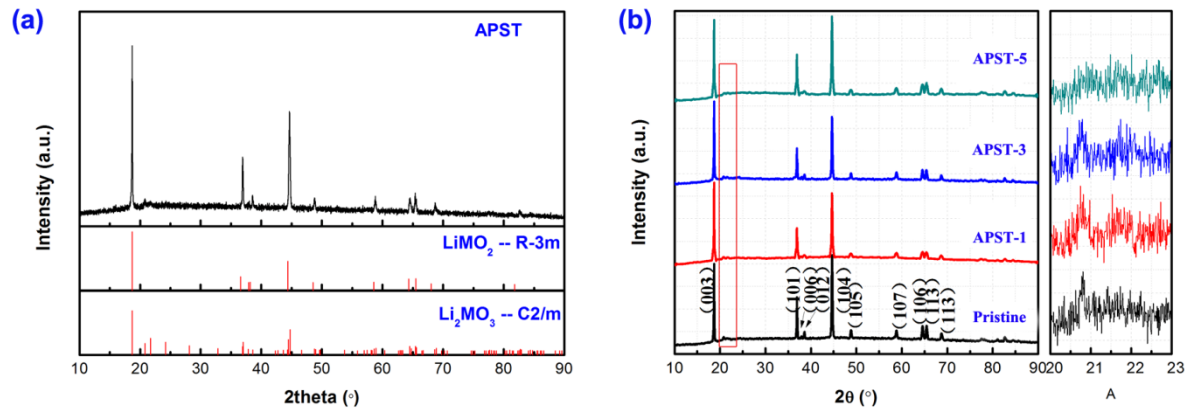

Figure S1. XRD pattern of APST and referred patterns of $LiMO_2$ with space group of R-3m and Li_2MnO_3 with space group of C 2/m.

Table S1. Lattice parameters and intensity ratio of I(003)/I(104) obtained from XRD patterns.

	a(Å)	c(Å)	c/a	I(003)/I(104)
Pristine	2.8531	14.2293	4.9873	0.912
APST	2.8535	14.2438	4.9917	1.568
AST	2.8537	14.2433	4.9911	1.531

The surface modified sample APST shows typical crystalinity of the α-$NaFeO_2$ structure with space group R-3m (JCPDS code: 01-087-1563), and peaks around 21°~25° are consistant with the $LiMn_6$ which can be indexed to monoclinic unit cell C2/m (JCPDS code: 00-027-1252). APST shows no exstra peaks for mixed phases, but a better ordered layered structure and increased c/a ratio. However, the ratio of c/a and the value of $I_{(003)}/I_{(104)}$ of AST don't differ much from those of APST, which implies AST and AST have similar structure with each other.[1, 2] When APS is over employed, $I_{(003)}/I_{(104)}$ decreases a lot, and super latice peaks at 20°~25°become weaker, indicating the order of layered structure is destroyed, and an over amount of Li^+ should be pre-extracted from Li_2MnO_3.

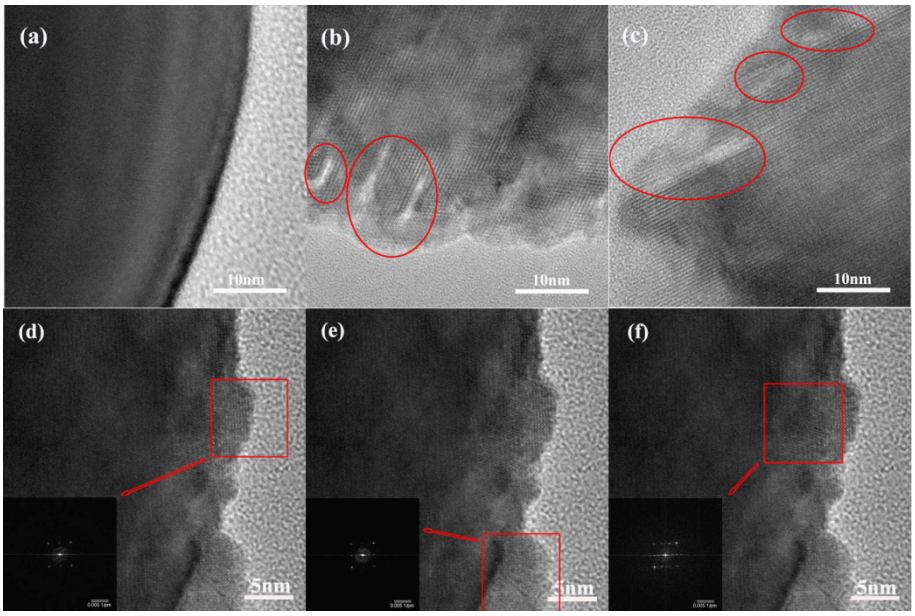

Figure S2. SEM images of pristine and modified $Li_{1.2}Ni_{0.13}Co_{0.13}Mn_{0.54}O_2$. (a) the pristine sample, (b) APST and (c)AST. HRTEM image of one single APST particle with corresponding FFT images to different nano-domain (d) , (e) and (f)

HRTEM image of the pristine $Li_{1.2}Ni_{0.13}Co_{0.13}Mn_{0.54}O_2$ show particle with clear and smooth edge, while AST and APST have rough edges as a result of surface modification reaction at the surcace, yielding cratches and pores. Such rough edge benifits the Li insertion and extraction process. The FFT images at local structure on one single particle of APST promote distinguishing the existence of different component more clearly. As can be seen in Fig S3 (d), (e) and (f), spinel outlayer can be somehow thinner than that given in the manuscript. So we conclude that when a smaller amount of APST is employed, a thinner spinel layer should be obtained.

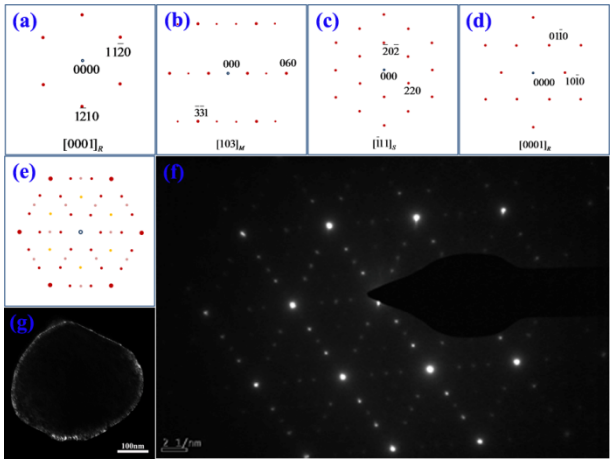

Figure S3. (a) Simulated SAED pattern of rhombohedral phase along [0001] zone axis. (b) Simulated SAED pattern of monoclinic phase along [103] zone axis. (c) Simulated SAED pattern of cubic spinel phase along [-111] zone axis. (d) Simulated SAED pattern of forbidden {10-10} reflection along [0001] zone axis. (e) The superimposition of the above simulated SAED patterns. (f) SAED pattern of APST. (g) dark field TEM image of APST particle.

The superimposition of simulated SAED pattern of rhombotherdral phase, spinel phase, monoclinic phase is exactely consistent with the practical SAED patern of APST, so it is doutless that such a modified material contains newly formed spinel outlayer and the original layered bulk. [3]

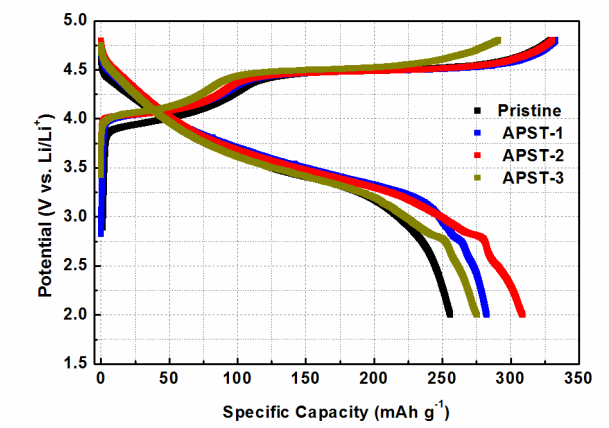

Figure S3. The charge/discharge curves of the pristine $Li_{1.2}Ni_{0.13}Co_{0.13}Mn_{0.54}O_2$ and APST that is treated to different degrees.

As can be seen in Figure S3, the pristine $Li_{1.2}Ni_{0.13}Co_{0.13}Mn_{0.54}O_2$, APST-1 and APST-2 all display charge capacity of about 330 mAh/g, while APST-3 show smaller charge capacity of 291.2 mAh/g. This difference in charge capacity should be attributed to the over loss of Li from $Li_{1.2}Ni_{0.13}Co_{0.13}Mn_{0.54}O_2$. When a small amount of APS is employed to surface modification on $Li_{1.2}Ni_{0.13}Co_{0.13}Mn_{0.54}O_2$, the increase of coloumbic efficiency should be contributed to two aspects, including the pre-extraction of Li^+ and the improvement of Li^+ conductivity . However, as the pre-fabricated spinel outlayer can facilitates the Li^+ intercalation afterwards, more Li^+ intercalates into the host material, which is the reason for the larger discharge capacity of APSTs than that of the pristine $Li_{1.2}Ni_{0.13}Co_{0.13}Mn_{0.54}O_2$. If APS is over used like APST-3, the obtained material can suffer the problem of reduced capacity. So it is important to note that such a surface modification should not be implemented to a large extent.[4]

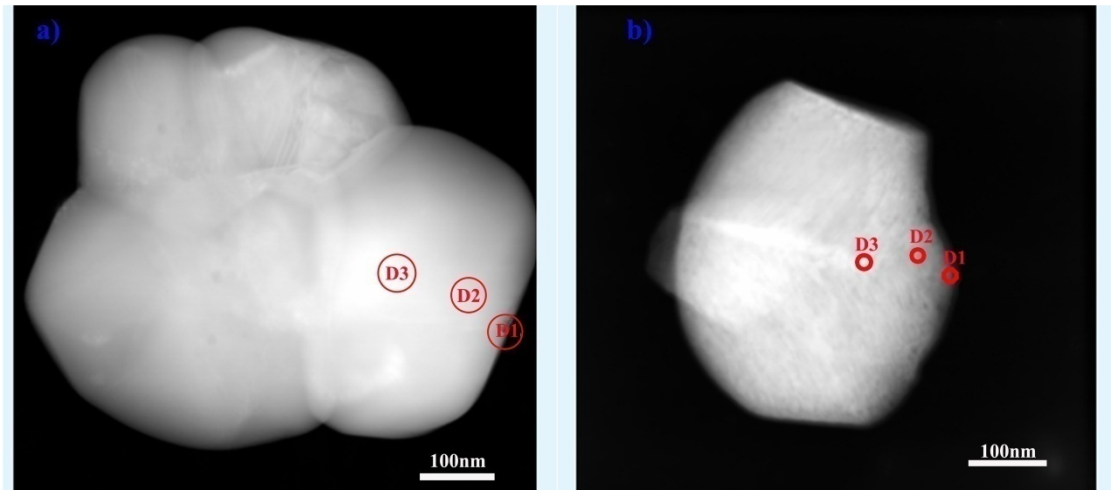

Figure S4. the HAADF-STEM images of (a) pristine and (b)AST

Table S2. EDS results of the content of transition metal elements at different nano-domain in a single particle (corresponding to Fig. S4 (a) pristine and (b) AST).

a) Pritine	Ni	Co	Mn
D1	13.08	13.18	73.75
D2	15.38	15.07	70.65
D3	15.08	14.71	69.61
b) AST	Ni	Co	Mn
D1	13.79	15.18	71.01
D2	14.53	15.45	70.01
D3	13.70	14.81	71.48

EDS results were collected from different nano-domains on one single particle of pristine $Li_{1.2}Ni_{0.13}Co_{0.13}Mn_{0.54}O_2$ and AST, respectively. The content of Ni/Co/Mn shown in Table S2 are in concert with different domain in Fig S4. The results show that there were no obvious loss of Colbat in AST and the pristine $Li_{1.2}Ni_{0.13}Co_{0.13}Mn_{0.54}O_2$ other than APST. Hence the difference of the spinel outlayer of the pristine $Li_{1.2}Ni_{0.13}Co_{0.13}Mn_{0.54}O_2$, AST and APST.[5]

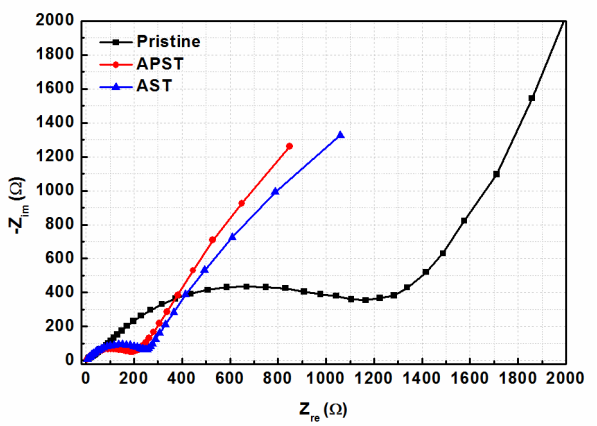

Figure S5. EIS of the pristine $Li_{1.2}Ni_{0.13}Co_{0.13}Mn_{0.54}O_2$, AST and APST at open circuit.

The nyquist plots of the pristine $Li_{1.2}Ni_{0.13}Co_{0.13}Mn_{0.54}O_2$, AST and APST at open circuit in Figure S5 suggests similar process in AST and APST. But the sloping line at low frequency which corresponds to Z_w infers difference in diffusion of lithium ion in the solid electrode)[6]

Table S3. Surface resistance (Rs) and charge transfer resistance (Rct) of ther pristine $Li_{1.2}Ni_{0.13}Co_{0.13}Mn_{0.54}O_2$, AST and APST after the first cycle and 200 cycles.

	After 1st cycle		After 200 cycles	
	Rs(ohm)	Rct(ohm)	Rs(ohm)	Rct(ohm)
Pristine	266.5	16326.1	112.1	11372.9
APST	81.4	1223.4	82.7	1267.2
AST	118.4	1663.5	45.7	10195.1

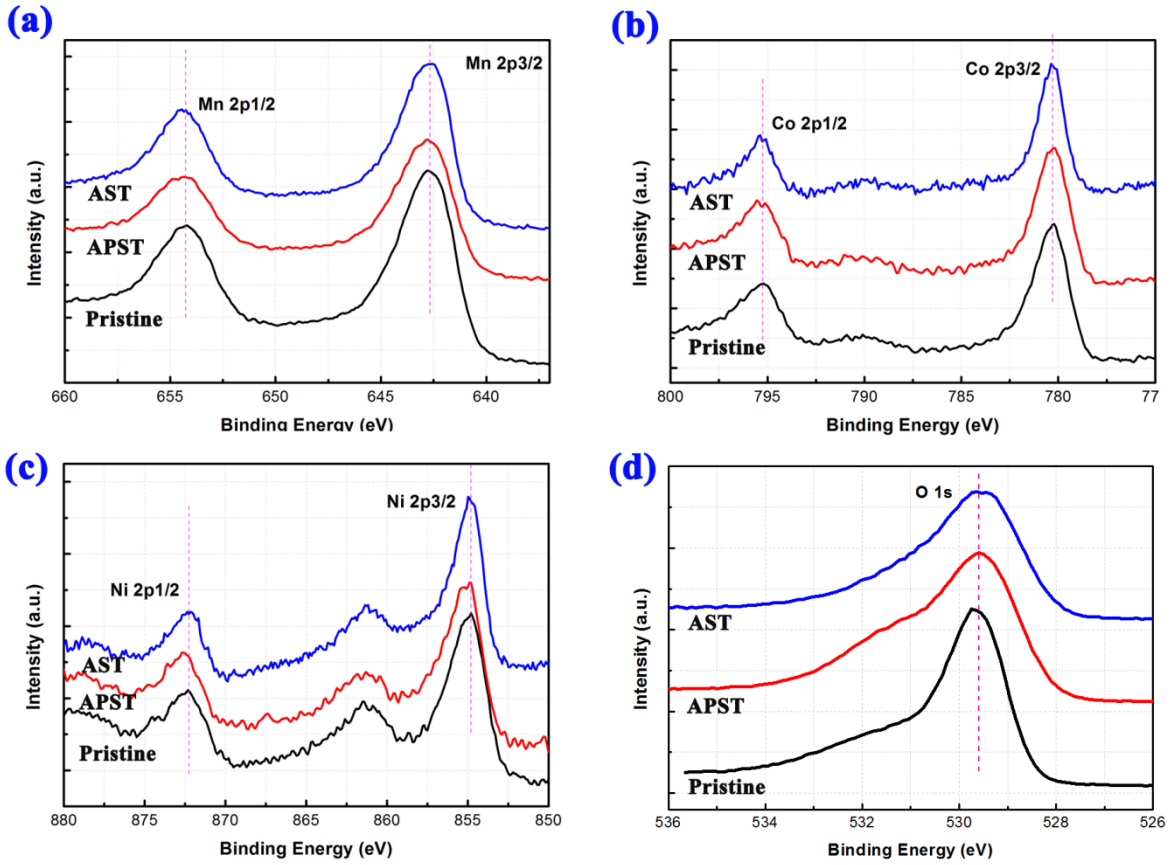

Figure S6. XPS spectra of the pristine $Li_{1.2}Ni_{0.13}Co_{0.13}Mn_{0.54}O_2$, APST and AST samples, (a) Mn2p, (b) Co2p, (c) Ni2p and (d) O1s

The XPS results in Firgure S6 show little difference in Mn and Co spectra of the pristine $Li_{1.2}Ni_{0.13}Co_{0.13}Mn_{0.54}O_2$ and AST and APST. In the Ni2p spectrum, there can be seen a peak shift towards higher binding energy in APST differing from that of the pristine $Li_{1.2}Ni_{0.13}Co_{0.13}Mn_{0.54}O_2$ and AST, which indicates the reaction between APS and $Li_{1.2}Ni_{0.13}Co_{0.13}Mn_{0.54}O_2$ leading to a Ni oxidation rather than Mn and Co. In addition, there is no clear difference between the pristine $Li_{1.2}Ni_{0.13}Co_{0.13}Mn_{0.54}O_2$ and AST, meaning AS treatment doesn't bring change in transition metal element oxidation status.[7]

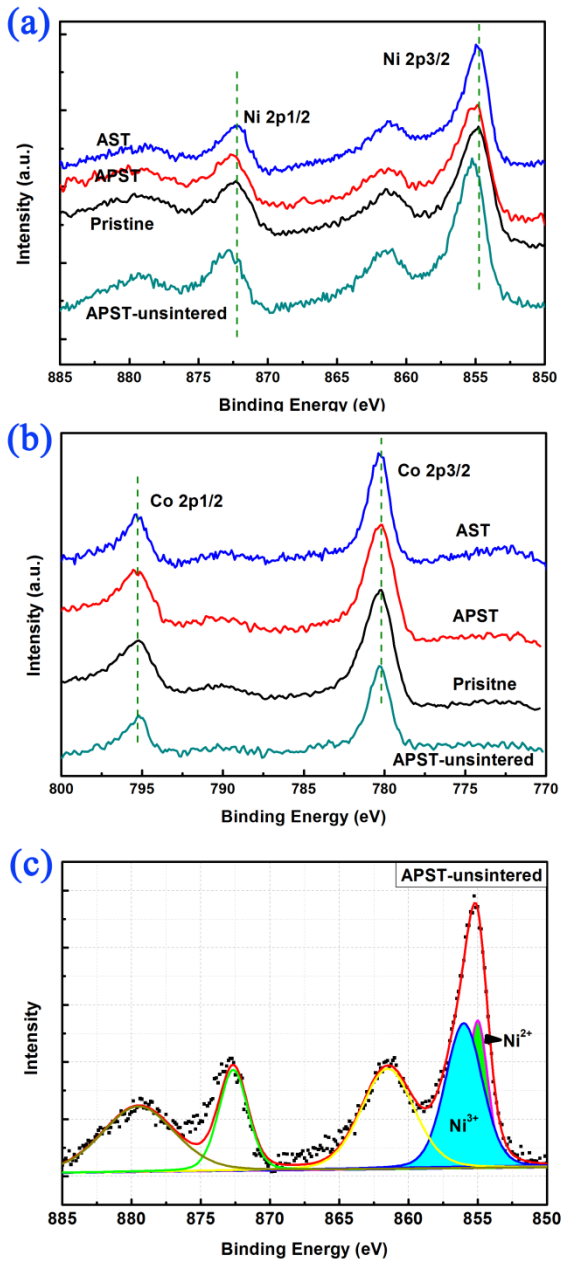

Figure S7. (a) Ni XPS spectra and (b) Co XPS spectra of the pristine $Li_{1.2}Ni_{0.13}Co_{0.13}Mn_{0.54}O_2$, APST,AST and unsintered APST samples, and (c) Ni fitting spectrum of unsintered APST.

Although we are not very clear about the virtual reaction mechanism between APS and Li1.2Ni0.13Co0.13Mn0.54O2 in the hydrothermal process, Ni is oxidized during the hydrothermal process, and Co in the particle is still trivalent. The XPS data of Ni spectrum and Co spectrum given in Figure S6 and Figure S7 confirmed that a large amount of Ni at the surface of APST is oxidized during the hydrothermal process rather than in the post calcination, while Co remains trivalent in the particle.

Table S4. Comparison on our results with other study on surface modification on Li-rich cathode materials.

	1st Charge/discharge capacity(mAh/g)	Coloumbic efficiency	Capacity retention	Capacity at 1C (mAh/g)	Capacity at 10C (mAh/g)	Capacity at 30C (mAh/g)
Zheng et al[8]	200-220/200 (2-4.8V)	91-100%	90%(after 50 cycles)	80~120	--	--
Han et al[3]	304/281 (2-4.6V)	92.4%	~92%(after 50cycles)	210	--	--
ours	330.5/308.7 (2-4.8V)	93.4%	~100%(after 200 cycles)	247	169	68.2

References:

1. J. Zheng, X. Wu and Y. Yang, *Electrochim. Acta*, 2013, 105, 200-208.
2. M. S. Zheng, J. J. Chen and Q. F. Dong, *Advanced Materials Research*, 2012, 476, 676-680.
3. S. Han, B. Qiu, Z. Wei, Y. Xia and Z. Liu, *J. Power Sources*, 2014, 268, 683-691.
4. Y. Chen, K. Xie, C. Zheng, Z. Ma and Z. Chen, *ACS Appl. Mat. Interfaces*, 2014.
5. G. Zhong, Y. Wang, Y. Yu and C. Chen, *J. Power Sources*, 2012, 205, 385-393.
6. J. Liu and A. Manthiram, *J. Mater. Chem.*, 2010, 20.
7. B. Song, H. Liu, Z. Liu, P. Xiao, M. O. Lai and L. Lu, *Scientific Reports*, 2013, 3.
8. J. Zheng, S. Deng, Z. Shi, H. Xu, H. Xu, Y. Deng, Z. Zhang and G. Chen, *J. Power Sources*, 2012.